

A NEWLY-RECOGNISED GALACTIC SUPERNOVA REMNANT WITH SHELL-TYPE AND FILLED-CENTRE FEATURES

Peter J. Barnes (Astronomy Department, University of Illinois, 1011 West Springfield Ave., Urbana, Illinois 61801-3000, USA) and

A. J. Turtle (School of Physics, University of Sydney, New South Wales 2006, Australia)

Introduction

While the number of galactic supernova remnants (SNRs) now known is fairly large (>150), the subset among these that are known to resemble the Crab Nebula is still distressingly small, about 15 or so (Green, 1984). Thus any object that can be unambiguously included in this exclusive club forms a valuable addition to our knowledge of this class. We report here observations of a newly recognised nonthermal galactic object, G18.94-1.06, having all the hallmarks of the classical shell-type SNRs, while also appearing to have a filled-centre component located inside the shell. Among the known Crab-like remnants, about one third show this dual nature (Green, 1984). This diagnosis of G18.94-1.06 is supported mainly by the variations in spectral index α ($S_{\nu} \propto \nu^{\alpha}$) across the source, as seen between the two observation frequencies, 408 MHz and 5.0 GHz.

Observations

In a study begun in 1980 and completed in 1985 (Barnes and Turtle, in preparation), several areas of the galactic plane were selected for detailed analysis using the results of two galactic plane continuum surveys: one at 408 MHz (Green, 1974), and the other at 5.0 GHz (Haynes *et al.*, 1978; 1979). The telescopes, observations and data reduction procedures will be described more fully in the above report. In these selected areas of the plane, over 100 separate objects were studied, including many apparent HII regions, SNRs, and extragalactic sources. Most of the 22 apparent SNRs are new candidates. Very early in this investigation, it was realised that G18.94-1.06 is one of the best new SNR candidates in this group, based on its morphology, size, brightness and spectral index. Fig. 1 shows the SNR as it was observed at 408 MHz with the 1.6 km cross-type radiotelescope at the Molonglo Observatory, near Hoskinstown, New South Wales, while Fig. 2 depicts its appearance as seen at 5 GHz with the 64 m dish near Parkes, New South Wales.

Note that at both frequencies the SNR is perched on the uneven background of the galactic plane, which hinders the derivation of the source parameters. After subtracting a sloping baseplane from each map, we obtain the following integrated flux densities: 58 ± 9 Jy at 408 MHz, and 23 ± 6 Jy at 5 GHz. Thus the overall spectral index for the SNR between these two frequencies is $\alpha = -0.37 \pm 0.17$. This value is intermediate between those typical of shell-type SNRs ($\alpha = -0.45$; Clark and Caswell, 1976) and filled-centre SNRs ($\alpha = -0.28$; Caswell,

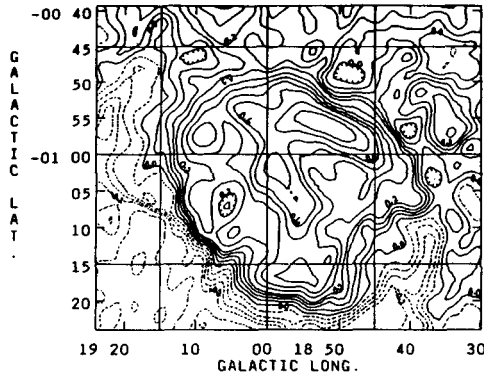


Figure 1: Map of G18.94 - 1.06 at 408 MHz before convolution and baseplane subtraction. Contour levels are at -0.4 -0.3, -0.2 (labelled), -0.15, -0.1, -0.05, 0.0 (labelled), 0.05, 0.1, 0.15, 0.2 (labelled), 0.3, 0.4, 0.5, 0.6 (labelled), 0.8, and 1.0 Jy/beam. Negative contours are shown as dashed lines. The angular resolution is 2'86 (R.A.) x 3'09 (Dec.), and so 1 Jy/beam = 272 K.

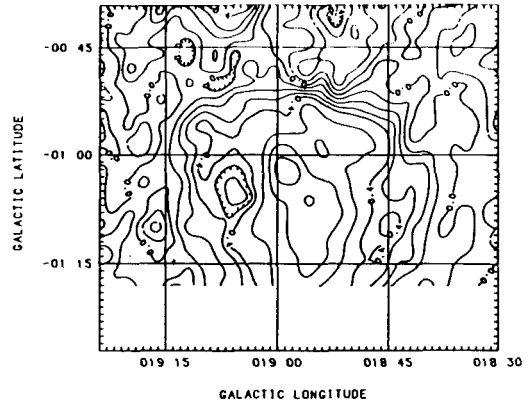


Figure 2: Map of G18.94 - 1.06 at 5 GHz after a sloping baseplane has been subtracted. Contour levels are at -0.4 (labelled), -0.3 (dashed), -0.2 (dashed), -0.1 (dashed), 0.0 (labelled), 0.1, 0.2, 0.3, 0.4 (labelled), 0.6, 0.8 and 1.0 Jy/beam. The angular resolution is 4'4 (R.A.) x 4'1 (Dec.), and so 1 Jy/beam = 0.750 K.

1979). Comparison with other observations amplifies this peculiarity: Altenhoff *et al.* (1970) measured flux densities at 1.4, 2.7 and 5.0 GHz of 42, 27 and 28 Jy respectively, while Fürst *et al.* (1985) obtained ($\pm 10\%$) 32.9, 27.4, 23.8 and 14.6 Jy at 1.42, 2.695, 4.75 and 10 GHz respectively. Thus, while these data are consistent with our flux densities and spectral index, a more careful inspection of the spectrum (Fig. 3) suggests a flattening of the spectral index towards higher frequencies (i.e., above 1.4 GHz), although the measurement at 10 GHz (14.6 Jy), if confirmed, would suggest a re-steepening of the spectrum beyond 5 GHz, to $\alpha \sim -0.66$.

Discussion

An explanation of this behaviour may be found in the detailed structure of the source as revealed in the maps (Figs. 1,2). G18.94-1.06 shows a definite, bright shell structure around most of its perimeter at 408 MHz, and so the classification as a SNR would seem to be a good one. However, the appearance at 5 GHz, while showing some shell-like features, is dominated by a brighter patch near the middle of the SNR, and this Crab-like blob has its counterpart at 408 MHz. The object's spectrum can now be explained as follows. At lower frequencies the shell part of the remnant dominates the emission, and it gives a value for the spectral index typical of shell-type SNRs. At higher frequencies, however, the central, flatter-spectrum part of the SNR dominates over the fainter shell, thus giving rise to the observed spectrum.

Because such a clear combination of Crab-like and classical SNR features would make G18.94-1.06 a valuable contribution to the list of known SNRs, one would like to confirm the spectral index variations across it in a more quantitative manner. To this end, the 408 MHz map was convolved to the resolution of the 5 GHz map and a spectral index map was formed (Fig. 4). As was suspected, we see that the SNR has $\alpha \sim -0.5$ to the north and east, typical of SNR shells, while towards its centre the spectral index drops to ~ -0.25 , close to the canonical

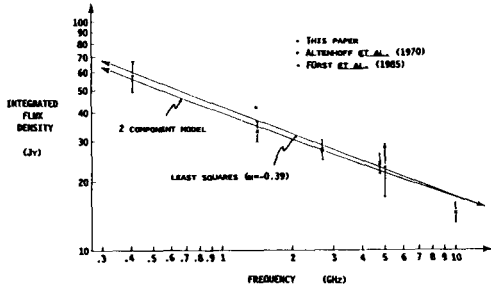


Figure 3: The radio spectrum of G18.94-1.06

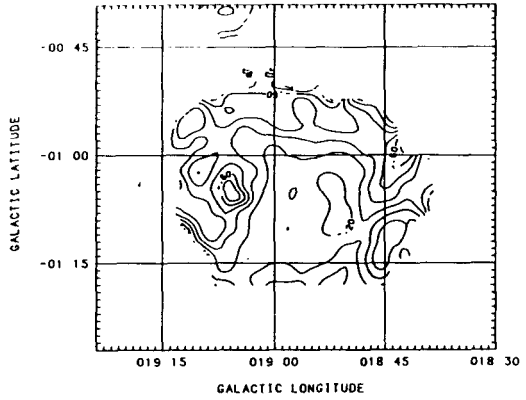


Figure 4: Spectral index map of G18.94 - 1.06 between the observation frequencies 408 MHz and 5 GHz. The spectral index has been calculated only where the signal in the convolved, subtracted 408 MHz map exceeded 30 mJy/beam, and where the signal in the subtracted 5 GHz map exceeded 50 mJy/beam. The gap at the south end of the map is due to lack of data at 5 GHz. The contour levels are in steps of 0.10 in spectral index, from -0.80 to -0.10; labelled contours are at -0.60 and -0.20.

filled-centre value. We may fit the integrated spectrum by a 2 component model, S_ν (Jy) = $33 (\nu_{\text{MHz}}/408)^{-1/2} + 23 (\nu_{\text{MHz}}/408)^{-1/4}$. This curve is shown in Fig. 3, along with a single component least squares fit.

Thus the case for G18.94-1.06 being a new member of the class of dual component SNRs appears to be a strong one. It could be confirmed further by detecting significant radio polarisation in the Crab-like component or the bright parts of the shell (a characteristic of both types of SNR; Weiler and Shaver, 1978) and/or by seeing the central blob as an X ray nebula. In fact, recent observations at 4.75 GHz have shown that both the central blob and the bright, northern edge of the shell are linearly polarised by up to 10% of the point-to-point emission, although the integrated polarisation is only 2.5% at this frequency (Fürst *et al.*, 1985). Hence the flatter spectrum in the middle cannot be explained by an unpolarised thermal contribution to the radio emission from an HII region.

PARAMETERS FOR G18.94-1.06

OBSERVED:

Major axis	35 arcmin
Minor axis	31 arcmin
Flux density S_{408}	58 Jy
Mean surface brightness Σ_{408}	$0.80 \times 10^{-20} \text{ W m}^{-2} \text{ Hz}^{-1} \text{ sr}^{-1}$

DERIVED:

	CL	MTLD
Distance d	4.5 kpc	3.4 kpc
Diameter D	43 pc	33 pc
Height above plane z	-82 pc	-63 pc
Age t	11300 yr	2200 yr
Mean expansion velocity V	1900 km s ⁻¹	7300 km s ⁻¹

The table presents the observed and derived data for the SNR. The first column of derived parameters (labelled "CL") was obtained using the Σ -(D,z) and related relationships of Caswell and Lerche (1979). An alternative approach to deriving SNR parameters was presented by Mills *et al.* (1984): this approach yields the quantities in the second column (labelled "MTLD"). Note that both distance scales give roughly the same distances and dimensions for the SNR, but that the two age estimates are mutually incompatible. Either distance scale would place G18.94-1.06 somewhere between the Scutum and Sagittarius spiral arms of the galaxy, leading us to expect the SNR to be very faint or invisible at optical wavelengths, due to extinction.

As a final note, we see that at both frequencies the Crab-like component appears extended in roughly the direction of the long axis of the remnant (about 30° inclination to the galactic plane). The obvious question is then: is the central component still interacting with the shell? Fürst *et al.*'s (1985) interpretation, that this source represents not a SNR but a new class of object produced by an accreting binary system, is now seen to be unnecessary, as the low-frequency data especially show that G18.94-1.06 resembles a SNR very closely. Although their model for the centre might yet prove to be relevant, their misinterpretation of the SNR nature of G18.94-1.06 is seen to be the result of a lack of high-resolution low-frequency data. Even higher resolution observations of this fascinating radio source should prove to be enlightening.

We would like to thank Drs. R.F. Haynes, J.L. Caswell and L. Newton for making the Parkes 5 GHz galactic plane survey data available to us.

References

- Altenhoff, W.J., Downes, D., Goad, L., Maxwell, A. & Rinehart, R. Astr. Astrophys. Suppl. (1970) 1, 319.
- Caswell, J.L. Mon. Not. R. astr. Soc. (1979) 187, 431.
- Caswell, J.L. & Lerche, I. Mon. Not. R. astr. Soc. (1979) 187, 201.
- Clark, D.H. & Caswell, J.L. Mon. Not. R. astr. Soc. (1976) 174, 267.
- Fürst, E., Reich, W., Reich, P., Sofue, Y. & Handa, T. Nature (1985) 314, 720.
- Green, A.J. Astr. Astrophys. Suppl. (1974) 18, 267.
- Green, D.A. Mon. Not. R. astr. Soc. (1984) 209, 449.
- Haynes, R.F., Caswell, J.L. & Simons, L.W.J. Aust. J. Phys. Astrophys. Suppl. (1978) 45.
- Haynes, R.F., Caswell, J.L. & Simons, L.W.J. Aust. J. Phys. Astrophys. Suppl. (1979) 48.
- Mills, B.Y., Turtle, A.J., Little, A.G. & Durdin, J.M. Aust. J. Phys. (1984) 37, 321.
- Weiler, K.W. & Shaver, P.A. Astr. Astrophys. (1978) 70, 389.